The GABAB receptor agonist STX209 reverses the autism-like behaviour in an animal model of autism induced by prenatal exposure to valproic acid

SHUCAI JIANG[1*], LIFEI XIAO[1*], YU SUN[1*], MAOTAO HE[2], CAIBIN GAO[1], CHANGLIANG ZHU[1], HAIGANG CHANG[1], JIANGWEI DING[1], WENCHAO LI[1], YANGYANG WANG[1], TAO SUN[1] and FENG WANG[3,1]

[1]Ningxia Key Laboratory of Craniocerebral Disease, Incubation Base of National Key Laboratory, Ningxia Medical University, Yinchuan, Ningxia 750004; [2]Department of Diagnostic Pathology, School of Basic Medical Sciences, Weifang Medical University, Weifang, Shandong 261053; [3]Department of Neurosurgery, The First Affiliated Hospital, Zhejiang University School of Medicine, Hangzhou, Zhejiang 310006, P.R. China

Received December 20, 2021; Accepted February 16, 2022

DOI: 10.3892/mmr.2022.12670

Abstract. Autism spectrum disorder (ASD) is a lifelong neurodevelopmental condition characterized by impaired social interaction, compromised communication, and restrictive or stereotyped behaviours and interests. Due to the complex pathophysiology of ASD, there are currently no available medical therapies for improving the associated social deficits. Consequently, the present study investigated the effects of STX209, a selective γ-aminobutyric acid type B receptor (GABABR2) agonist, on an environmental rodent model of autism. The mouse model of autism induced by prenatal exposure to valproic acid (VPA) was used to assess the therapeutic potential of STX209 on autism-like behaviour in the present study. This study investigated the effects of STX209 on VPA model mice via behavioral testing and revealed a significant reversal of core/associated autism-like behavior, including sociability and preference for social novelty, novelty recognition, locomotion and exploration activity and marble-burying deficit. This may be associated with STX209 correcting dendritic arborization, spine density and GABABR2 expression in hippocampus of VPA model mice. However, expression of glutamic acid decarboxylase 65/67 in the hippocampus were not altered by STX209. The present results demonstrated that STX209 administration ameliorated autism-like symptoms in mice exposed to VPA prenatally, suggesting that autism-like symptoms in children with a history of prenatal VPA exposure may also benefit from treatment with the GABABR2 agonist STX209.

Correspondence to: Professor Feng Wang, Department of Neurosurgery, The First Affiliated Hospital, Zhejiang University School of Medicine, Hangzhou, Zhejiang 310006, P.R. China
E-mail: nxwwang@163.com

Professor Tao Sun, Ningxia Key Laboratory of Craniocerebral Disease, Incubation Base of National Key Laboratory, Ningxia Medical University, 1160 Shengli Street, Yinchuan, Ningxia 750004, P.R. China
E-mail: suntao_nxmu@163.com

*Contributed equally

Key words: valproic acid, autism spectrum disorder, autism, STX209, γ-aminobutyric acid type B receptor 2

Introduction

Autism is a lifelong neurodevelopmental disorder and one of the most severe mental health disorders in childhood. In 2013, the diagnosis of autism and several other disease categories were incorporated into the singular diagnostic category of autism spectrum disorder (ASD) (1,2). Autism has a poor prognosis and a high disability rate, which greatly increases family and social burdens (3). Currently, there is no cure available for ASD, and its aetiology comprises environmental and genetic variables. Rodent models based on genetic factors have been widely used in preclinical research, such as the Fmr1-knockout mouse model, the BTBR T + tf/J mouse model, the Nlgn-3 and Nlgn-4-mutant mouse model, the Shank-mutant mouse model and the $Tsc2^{+/-}$ mouse model (4). While ASD has a strong genetic component, a wide range of environmental factors, including prenatal exposure to intrauterine infections; drugs, such as valproic acid (VPA) and thalidomide; or toxicants, such as organophosphate insecticides or heavy metals, are also thought to confer ASD susceptibility (4-7). VPA, a broad-spectrum antiepileptic drug, has been used worldwide to treat certain types of epileptic encephalopathy, as well as bipolar disorder and migraine; exposure to VPA during pregnancy has been demonstrated to increase the likelihood of autism in children (5-8). The VPA mouse model, which has stable face, construct and predictive validity, is a robust model of ASD that has been used extensively to increase understanding of the neurobiology underlying autistic behaviour and to screen novel drugs for autism treatment (5,8-10).

Nevertheless, the underlying biological mechanism of ASD remains undetermined, and consequently, no specific therapeutic strategy has yet been established. There are currently a few pharmacological treatments available, such as risperidone and aripiprazole, which help relieve some symptoms, such as aggression, self-injurious behaviour and anxiety, but do not address the core characteristics of autism, such as impaired social interaction and restrictive interests (8,11-13).

There is much evidence that the γ-aminobutyric acid type B (GABA)ergic system is a potential therapeutic target for core ASD symptoms (13,14). GABAergic system dysregulation is common in clinical cases of ASD and has been proposed as a cause of excitation-inhibition (E-I) imbalance (15-21). GABAergic system dysregulation and E-I imbalance are commonly observed in rodent models of autism, and correction of these disorders by pharmacological interventions can normalize core autistic-like phenotypes in these animals (22,23). Notably, previous studies have suggested that VPA rodent models exhibit GABAergic signalling dysfunction, extensive alterations in neuronal morphology and local neocortical microcircuit disorder (24-33). The GABAB receptor (GABABR2) agonist STX209 is an exploratory drug comprising the single, active R-enantiomer of baclofen (R-baclofen) and has the advantage of being a biologically defined and active enantiomer (34,35). The potential of STX209 to treat autism symptoms in VPA model mice has attracted our attention.

Previous studies have suggested that the exploratory medicine STX209 (arbaclofen), a selective agonist of GABABR2, may improve autism-associated behaviours in rodent models with certain genetic defects (36-40); for example, intraperitoneal/oral administration of STX209 was shown to exhibit favourable effects on Fmr1-knockout mice (36,41). Although the results of the majority of clinical trials have supported the therapeutic effects of STX209 (42-45), the phase III clinical trial of R-baclofen for the treatment of fragile X syndrome with the ASD phenotype was prematurely terminated due to lack of efficacy (46). These findings indicated that GABABR2 agonists may be effective for some subgroups of patients with ASD but not for all; therefore, STX209 may have the potential to improve autism-like symptoms in some unknown subgroups of patients with ASD. The present study focused on children with ASD caused by environmental factors, such as VPA, have attracted our attention. To the best of our knowledge, there are no relevant reports of STX209 treatment in VPA-exposed mice.

The present study hypothesized that GABABR2 may participate in the occurrence of the core behavioural symptoms of ASD and that chronic administration of STX209 could reverse autism-like behaviour in an animal model of autism induced by prenatal exposure to VPA. A series of behavioural experiments was designed to evaluate the therapeutic potential of STX209 on autism-relevant behavioural phenotypes in VPA-exposed mice and the possible mechanism was evaluated.

Materials and methods

Ethics approval. The present study was a preclinical study using a rodent model. All experimental operations and tests were performed at the Key Laboratory of Craniocerebral Disease, Ningxia Medical University (Yinchuan, China). All mice were handled according to protocols approved by the Institutional Animal Care and Use Committee of Ningxia Medical University (IACUC Animal Use Certificate no. 2019-152). All efforts were made to minimize the number of animals used and their suffering.

Animals. Breeding pairs of C57BL/6J mice (age, 10 weeks; weight of female mice, 20-25 g; weight of male mice, 22-25 g) were purchased from Ningxia Medical University Laboratory Animal Center and housed in a conventional mouse vivarium at the Feeding Unit of Ningxia Medical University Craniocerebral Laboratory. The total number of mice purchased for mating was 30 (10 males and 20 female). Each male mouse was housed in a single cage and female mice were housed in pairs(random allocation). Standard rodent chow and tap water were available *ad libitum*. All mice were maintained under standard laboratory conditions at 22±2˚C with 50±10% relative humidity and under a 12-h light/dark cycle. A total of 1 week after entering the feeding unit, precontact between male and female mice was conducted for 3 days to regulate the fertility cycle; when the female mice were in a proestrus state, the animals were allowed to mate overnight (5 p.m. to 8 a.m. the next day). Detection of a vaginal plug in female mice was designated as half a day of pregnancy. The pregnant mice were then housed separately and divided into vehicle- and VPA-treated groups. Because of precontact (male and female mice were housed in the same cage, but separated by isolation nets to prevent mating), female pregnancy and pup birth could be concentrated within a 3-day period. In the present study, 10 male mice and 20 female mice were used for mating. After the offspring were weaned (postnatal day 21, P21), the parent mice were euthanized by CO_2 using a Laboratory Animal Asphyxiator (SMQ-II; Shanghai Minly Lab Hi-tech Development Co., Ltd.) (47). The following model of general euthanasia was used: Increased CO_2 concentration from 0-90%/5-6 min; the CO_2 replacement rate was 60% CO_2/min in a chamber, according to the AVMA Guidelines for the Euthanasia of Animals, 2020 (48). Death was confirmed by the absence of a heartbeat and breathing.

Prenatal VPA exposure. VPA (MilliporeSigma) was dissolved in 0.9% normal saline (NS) at a 10 mg/ml concentration. Prenatal VPA exposure was induced according to a novel method first described by Zheng *et al* (49); female mice in the VPA-treated group received two doses of 300 mg/kg VPA on embryonic day 10 (E10) and E12 (Fig. 1A); female mice in the control group were injected with the same amount of NS on these days. Prior to initiation of this experiment, several relevant studies were consulted; most reports of this rodent model administered a single injection of VPA at doses ranging from 300 to 800 mg/kg between E9-12.5, and 500 mg/kg was the usual dose (8,24,50). We were cautious about reducing the dose, as this may increase the risk of an imperfect phenotype of VPA model mice and it was unclear whether this would affect their autism-like behaviour. Increased doses may result in an increase in the rate of miscarriage; this does not conform to animal theory.

The new method of administration is closer to the pathological process that induces ASD after repeated administration of VPA in the clinic as previously described (49). Foetal mice receive double administration (double blow) during the critical period of brain development, and the blows last longer and are more stable. Compared with the traditional method, this will obviously cause more serious damage to the brain development of the offspring, and because low doses of VPA are applied at intervals, the new method is gentler on the pregnant mice (49). Clinically, the maximum dose of VPA medication for patients is 30 mg/kg, which is completely absorbed 1-4 h after medication, and reaches a peak value. It is mainly metabolized by the liver and excreted by the kidneys (49). According to the new method protocol, after birth, female mice raised their litters. Male offspring were weaned on P21 and were labelled with ear tags. The ASD-related behaviour of male VPA model mice has been reported to be more stable than that of female VPA model mice (5,10,51); therefore, only male offspring (all mice, n=56; prenatal VPA exposure groups contained VPA group and VPA + STX209 group, n=28; no prenatal VPA exposure groups contained CTRL group and CTRL + STX209 group, n=28; n=14/group) were used for subsequent experiments. The male offspring were administered isoflurane anaesthesia (4%) at approximately P60 and once it was confirmed they had been satisfactorily anaesthetized, they were sacrificed by decapitation (Fig. 1A). Female offspring did not enter the experimental process and were euthanized by CO_2 using a Laboratory Animal Asphyxiator after they were weaned (P21). The following model of general euthanasia was used: Increased CO_2 concentration from 0-90%/5-6 min. the CO_2 replacement rate was 60% CO_2/min in a chamber as aforementioned. Death was confirmed by the absence of a heartbeat and breathing. All male offspring from the same litter were equally distributed to the STX209 administration groups (CTRL+STX20 group, n=14; VPA+STX209 group, n=14) and the no administration groups (CTRL group, n=14; VPA group, n=14) to eliminate the litter effect (52).

Drug administration. STX209 (MedChemExpress) was administered intraperitoneally to CTRL+STX20 and VPA+STX209 group mice at a dose of 0.6 mg/kg in 0.9% NS twice a day from weaning (P21) until the end of the experiment (approximately P60) (Fig. 1A). The STX209 dose was selected based on the effective dose in neuropathy and children with ASD in experimental animal studies and clinical trials (36,41,42). Injections were given at 8:00 a.m. and 8:00 p.m.

Neurodevelopmental behaviour tests. To assess the success and efficiency of the modified method in generating the mouse model of VPA-induced autism, a battery of tests was designed and utilized to evaluate developmental milestones (24,53,54). The sequence and timing of the tests are shown in Fig. 1A. The day of onset was recorded and positive reflexes were confirmed the following day. Because sex of pups was hard to distinguish, we tested all pups in the VPA (n=61) and CTRL group offspring (n=39).

Surface righting reflex. Beginning on P5, all new-born mice were placed in the supine position on a board, and the first appearance of the surface righting reflex was defined as the ability of the pups to turn over to the prone position and stand with all four paws in contact with the board within 10 sec. All pups were checked and recorded every day until they all reached the standard.

Negative geotaxis reflex. Beginning on P5, pups were placed facing downwards on a rough wooden slope with a 30˚ incline, held there for 3 sec and then released. The ability of the pups to turn to face upwards (rotate 180˚) within 30 sec was assessed. The first day the animals appeared to successfully accomplish the task was recorded.

Air righting reflex. Pups were dropped naturally from the supine position onto soft bedding (30 cm high). A mouse was considered to exhibit a positive reflex if it landed in a normal prone position (belly facing downwards against the bedding). The test was started on P10.

Growth and development. The body weight (BW) and tail length (TL) of each mouse pup (male VPA pups: n=28, contained unpublished data; male CTRL pups: n=23, contained unpublished data) were recorded on days 21, 28 and 35 after birth. BW was measured by putting the mouse on a balance and reading the measurement after the mouse rested for 2 sec. Pups were weighed twice and the mean was calculated. Pup TL measurement started from the root of the tail and the length of the tail was measured in a straight state. The crooked tail of mice was observed easily after P10 in the VPA group (Fig. 1B).

Autism-related behaviour tests. The sequence and timing of the tests are shown in Fig. 1A. All behaviours of the animals were recorded using a computerized video tracking system (SMART 3.0; Panlab).

Social interaction test. Mice were tested in a three-chambered social approach apparatus as previously described with slight modifications (cages placed diagonally across chambers) (37,38). The test had two tested phases: i) The sociability phase (scene 1), in which an unfamiliar mouse (stranger 1) was placed inside a plastic cage in one of the side chambers, an empty cage was placed in the other chamber, and the test mouse was allowed to freely explore the apparatus for 5 min; and ii) the preference for social novelty phase (scene 2), in which a second unfamiliar mouse (stranger 2) was placed inside the cage in the opposite chamber and the test mouse was allowed to freely explore the apparatus for 5 min. The total time spent in each region and the time spent sniffing the stranger mouse and the empty cage were recorded. The social preference index (SPI) was calculated as follows: SPI=(time spent in the region containing stranger 2)/(time spent in the region containing stranger 1 + time spent in the region containing stranger 2) in scene 2. The test started at ~9:30 AM.

Novel object recognition task. The novel object recognition task was performed as previously reported (40,55) with slight modifications (clear distinction between white plastic bottle and black glass bottle, which were used as familiar and novel object, respectively). The animals were placed in

a box containing two identical objects (white plastic bottle) and allowed to explore for 5 min (scene 1). Subsequently, one object was replaced with a novel object (black glass bottle) and the animals were allowed to explore the objects for 5 min (scene 2) after an interval of 30 sec. The discrimination index (DI) was calculated as follows: DI=(time spent exploring the novel object)/(time spent exploring the novel object + time spent exploring the familiar object). The task started at ~9:30 AM.

Open-field task and open-field habituation task. The open-field boxes used for this assessment were made of wood (50.0x50.0x40.0 cm) and an overhead camera was used for automatic tracking of animal behaviours using SMART 3.0. The box was divided into two zones: An 'inner' zone (a 30x30 cm^2 central square) and an 'outer' zone (10 cm from the walls). The duration of the test was 10 min.

Inspired by a previous study (40), the open-field test was repeated at 24-h intervals and the same indexes [time travelled in the inner area, the distance travelled in the inner area and open-field exploration index (OFEI)] were measured for every mouse. OFEI was calculated as follows: OFEI=distance travelled in the inner zone/the total distance travelled. The task started at ~9:30 a.m.

Marble burying test. The marble burying test was performed as previously reported (36,37,50) with slight modifications. The tested mouse was placed in a black cage containing 16 marbles arranged in a 4x4 grid on clean rice husk bedding <5 cm in height. A mouse was placed in a standard mouse cage containing 16 marbles arranged in a 4x4 grid on clean rice husk bedding. The duration of the test was 10 min. Marbles with >75% of their surface buried in the bedding were counted and recorded. Digital images and videos of the marbles were captured during the test period. The numbers of buried marbles and burying actions (strong and obvious digging or burial movement) were counted from the digital images and videos by trained investigators (n=3) who were blinded to the group allocations and the mean result was rounded. The test started at approximately 09:30 p.m.

Golgi-Cox staining. Golgi staining is used to provide valuable information regarding the neural morphology and quantitative assessments such as dendritic spine number, dendritic length measurements (33). We used the Golgi-Cox staining method to observe the neuronal dendritic length and spine number of CA1, DG region of mice. After deep anesthesia was induced with isoflurane as aforementioned, the mice were decapitated, and the brains were removed and soaked in mixed AB liquid immediately (FD Rapid GolgiStain™ kit, NeuroTechnologies). After 3 weeks, brain tissues that were completely infiltrated with mixed AB liquid were sliced with a vibrating slicer (VT1000S; Leica, GmbH) and then brain slices were placed on the glass dish, soaked in liquid C. The thickness of each slice was 100 μm. After 5 days, slices were stained with mixed DE liquid (solution D:solution E:distilled water; 1:1:2) for 10 min, after which the slices were rinsed with distilled water, dehydrated with an ascending series of ethanol solution and cleared in xylene for >2 h. Finally, the slices were sealed on slides with neutral resin and dried in the dark.

Neurolucida 360 imaging and Sholl analysis. Z-stack images of neurons were captured using a Leica DM6 fluorescence microscope (Leica Microsystems GmbH). 3D reconstruction of neurons from the images and Sholl analysis were performed with Neurolucida 360 software (MBF Biosciences) on the Public Technology Platform of Zhejiang University (Hangzhou, China).

Dendritic spine analysis. Images of spines were obtained with the Extended Depth of Focus module of a Nikon orthotopic light microscope (Nikon Corporation). 3D dendritic spine images were combined into a plan view and the manual counting mode of ImageJ analysis software (National Institutes of Health, 2020 version) was used to evaluate the images. Spines were classified into subtypes based on the width and length of the spine by three investigators who were blinded to the group allocations and mean values were calculated.

Western blotting. Total proteins were extracted from the hippocampus of mice using the Protein Extraction Kit (cat. no. KGP2100; Nanjing KeyGen Biotech Co., Ltd.) and the protein concentration was measured using the BCA Protein Assay Kit (cat. no. KGP902; Nanjing KeyGen Biotech Co., Ltd.). Equal amounts of protein (60-80 μg/lane) were separated by SDS-PAGE on 8 or 10% gels and were then transferred to PVDF membranes. When the protein transfer was completed, membranes were blocked with 5% non-fat milk for 1 h in room temperature, followed by incubation for ~20 h at 4˚C with rabbit anti-GABABR2 (1:500; cat. no. ab230136), anti-glutamic acid decarboxylase (GAD)65/67 (1:500 cat. no. ab183999) and anti-GAPDH (1:1,000; cat. no. ab181602) antibodies. Subsequently, the membranes were washed with TBS-Tween (0.5%) three times (5 min/wash) and were further incubated with the corresponding goat anti-rabbit IgG secondary antibody (1:1,000; LI-COR Biosciences cat. no. P/N: 926-32211) for 2 h in room temperature. GAPDH served as an internal reference. Semi-quantification of bands was performed from optical density values using the Odyssey CLX instrument system (LI-COR Biosciences).

Statistical analysis. Data are expressed as the mean ± SEM. Statistical analysis was performed using GraphPad Prism 8.0 (GraphPad Software, Inc.). $P<0.05$ was considered to indicate a statistically significant difference. The BW and TL data were analysed using two-way mixed ANOVA [independent variables: Treatment (VPA or control) and time]. Neurodevelopmental behaviour test data were analysed using unpaired Student's t-test. Social interaction test, novel object recognition task, Golgi-Cox staining and western blotting data were analysed using two-way ANOVA [independent variables: Drug (STX209 or control) and treatment (VPA or control)]. Open-field test (task 1) and open-field habituation test (task 2) data were analysed using paired Student's t-test for comparing the differences between different tasks in the same group of mice and three-way mixed ANOVA for comparing the differences among groups of mice in the same task.independent variables: Drug (STX209 or control), treatment (VPA or control) and scene (1 or 2)]. Marble burying test data were analysed using Pearson correlation, linear regression analysis or two-way ANOVA [independent variables: Drug (STX209

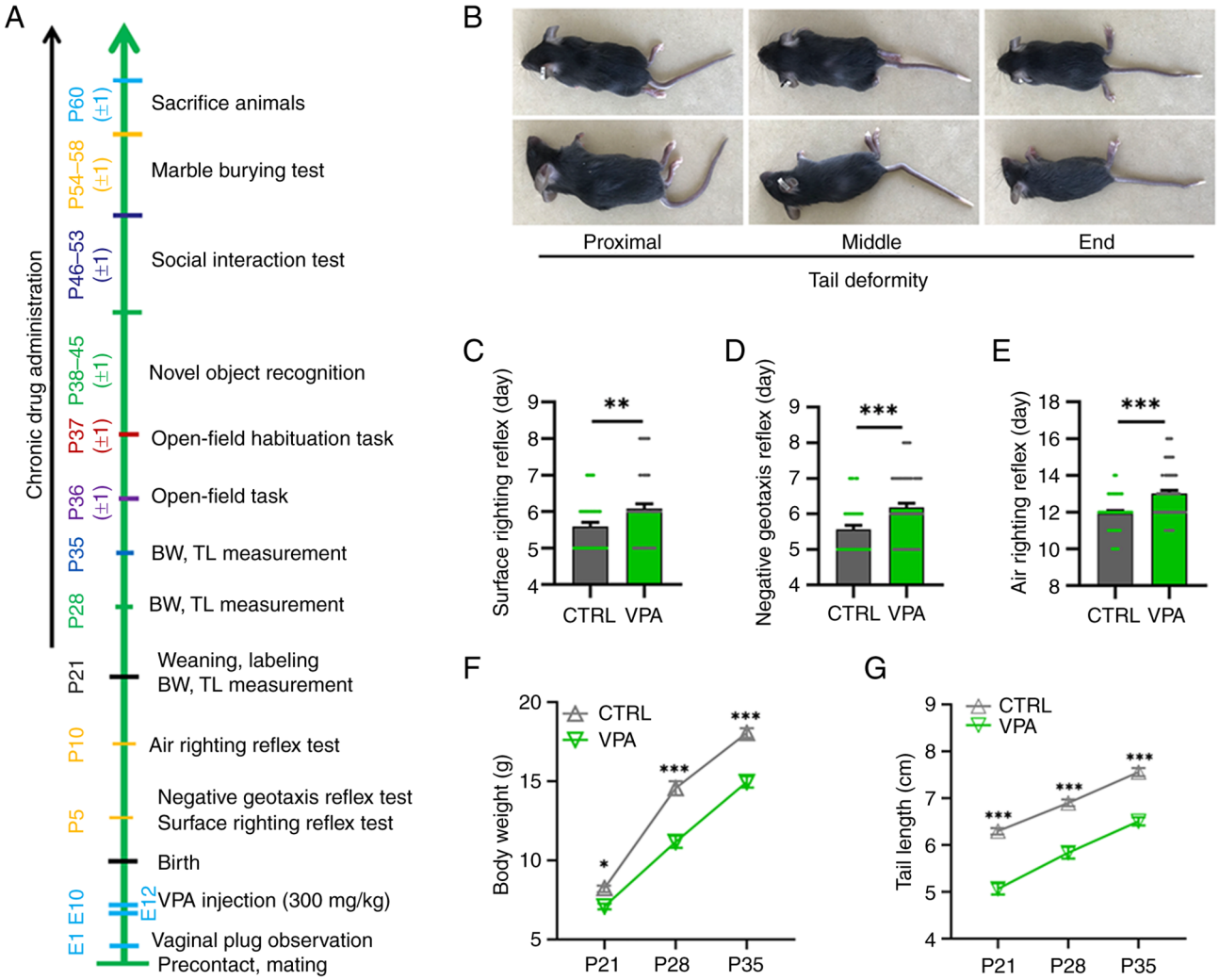

Figure 1. VPA model mice exhibit delayed nervous reflex development, delayed growth and tail malformations. (A) A representative timeline of the experimental approach. Mice were sacrificed ~60 days after birth for Golgi staining and western blotting. (B) Images of the prone and lateral positions of three VPA model mice with deformities in different parts of the tail. All VPA model mice exhibited tail malformation to different extents. VPA model pups (n=61, male pups and female pups) exhibited significantly longer latencies, including latencies to the first appearance of the (C) surface righting reflex, (D) negative geotaxis reflex and (E) air righting reflex, than CTRL pups (n=39, male pups and female pups) in the behavioural tests. **P<0.01, ***P<0.001 (Student's unpaired t-test). (F) BW and (G) TL of VPA model mice (n=28, only male offspring, contained unpublished data) were lower than those of CTRL mice from P21 to P35 (n=23, only male offspring, contained unpublished data). *P<0.05, ***P<0.001 (two-way mixed ANOVA followed by Bonferroni post hoc test). All data are presented as the mean ± SEM. BW, body weight; CTRL, control; E, embryonic day; P, postnatal day; TL, tail length; VPA, valproic acid.

or control) and treatment (VPA or control)]. All two-way and three-way mixed ANOVAs were followed by Bonferroni post hoc test to compare the differences among the groups.

Results

Tail malformations in VPA model mice. Neural tube defects (NTDs) can result from genetic mutations, malnutrition or exposure to teratogens during gestation (56). VPA is a known inducer of NTDs and causes a crooked tail phenotype (a mild NTD sign), which is often used as a sign of successful modelling in VPA rodent models of ASD (5,50,57). The crooked tail phenotype was observed in all VPA model mice in the present study, indicating successful induction of an ASD model (Fig. 1B).

VPA model mice exhibit delayed nervous reflex development. As shown in Fig. 1C-E, prenatal VPA-exposed mice exhibited significantly longer latencies in behavioural ontogeny compared with control mice, including the first appearance of the surface righting reflex (P=0.0084; Fig. 1C), negative geotaxis reflex (P=0.0007; Fig. 1D) and air righting reflex (P<0.0001; Fig. 1E). These results indicated that prenatal VPA exposure had a neurotoxic effect on offspring mice and that VPA model mice exhibited nervous reflex developmental defects in the present experiment.

Growth retardation in VPA model mice. The BW and TL of pups were measured every week between P21 and P35 (Fig. 1A). The BW of VPA mice was significantly smaller than that of control mice at P21-P35 (BW: P21, P=0.0429; P28, P<0.0001; P35, P<0.0001; Fig. 1F). The TL of VPA mice was also significantly shorter than that of control mice at P21-35 (P21, P<0.0001; P28, P<0.0001; P35, P<0.0001; Fig. 1G). These results indicated that VPA mice exhibited severe growth retardation postnatally.

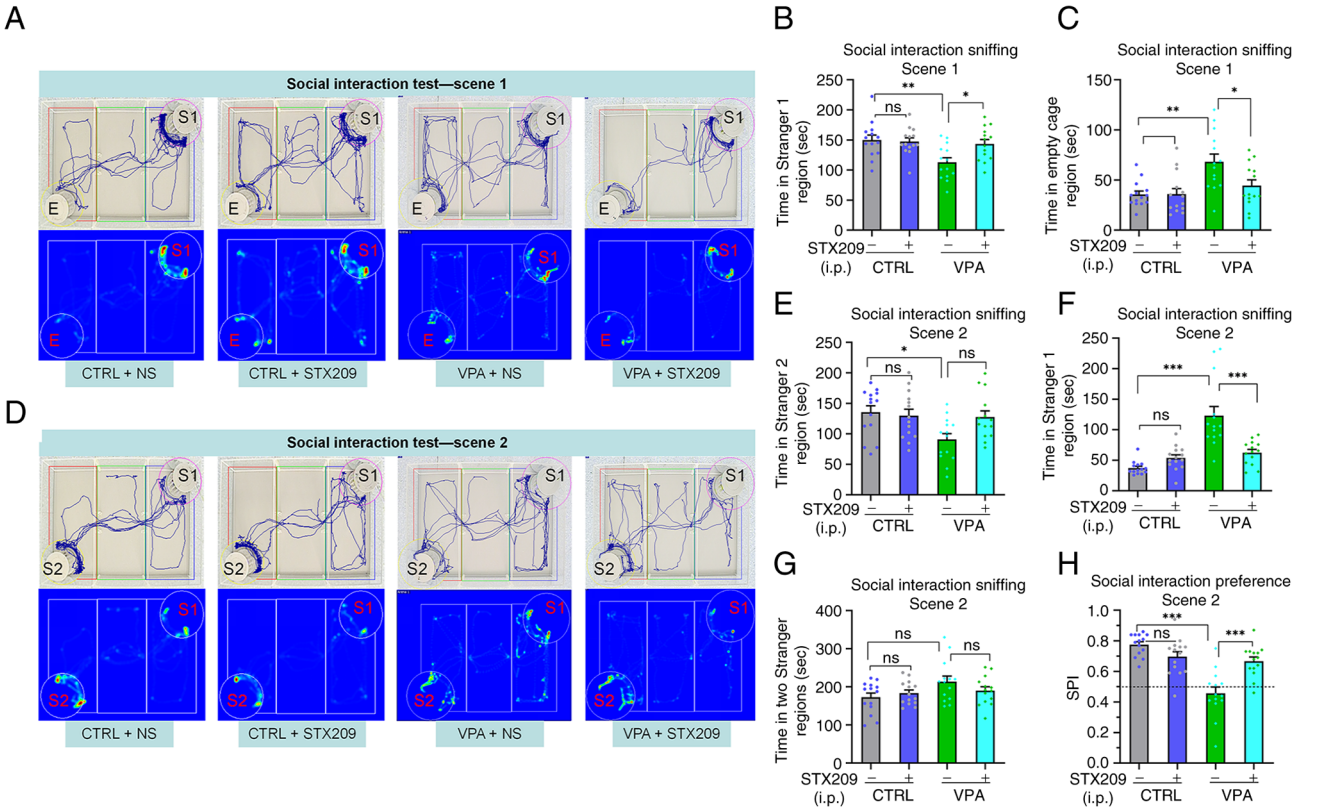

Figure 2. Treatment with STX209 ameliorates sociability deficits and preference for social novelty deficits in VPA model mice. (A) Representative trace and heatmap images from tested mice in scene 1 in the social interaction test (E, empty; S1, stranger 1). (B) Time that tested mice entered the region containing stranger 1 for sniffing in scene 1. (C) Time that tested mice entered the empty cage region for sniffing in scene 1. (D) Representative trace and heatmap images from tested mice in scene 2 in the social interaction test (E, empty; S1, stranger 1; S2, stranger 2). (E) Time that tested mice entered the region containing stranger 2 for sniffing in scene 2. (F) Time that tested mice entered the region containing stranger 1 for sniffing in scene 2. (G) Total time that tested mice entered the region containing stranger 2 and stranger 1 for sniffing in scene 2. (H) SPI of tested mice in scene 2. *P<0.05, **P<0.01, ***P<0.001 (two-way ANOVA followed by Bonferroni post hoc test). All data are presented as the mean ± SEM. Each group had 14 mice. CTRL, control; NS, normal saline; SPI, social preference index; VPA, valproic acid; ns, no significance.

STX209 ameliorates the sociability deficits of VPA model mice. During scene 1, sociability is defined as the propensity to spend time in the cage containing stranger 1 compared with time spent alone in the identical but empty opposite cage (4). The session indicates the interest in social cues of the tested mouse (4,58,59). The analysis results of the trace images and heat images showed (Fig. 2A), mice in the VPA group spent less time in the cage containing stranger 1 than mice in the control group (P=0.0044) and VPA + STX209 group (P=0.0280) in scene 1 (Fig. 2B). By contrast, in scene 1, mice in the VPA group spent more time in the empty cage region (control vs. VPA, P=0.0012; VPA vs. VPA + STX209, P=0.0323; Fig. 2C). These results revealed that VPA mice exhibited obvious sociability deficits and that STX209 ameliorated these deficits.

STX209 ameliorates the preference for social novelty deficits of VPA model mice. During scene 2, preference for social novelty is defined as the propensity to spend time with a new stimulus rather than with the same stimulus encountered in scene 1 (4,58,59). The session indicates the interest in new social cues of the tested mouse.

In scene 2 (Fig. 2D), VPA model mice spent less time in the cage containing stranger 2 than mice in the control group (P=0.0175; Fig. 2E); in addition, the average time the VPA group spent in the cage containing stranger 2 was less than that of the VPA + STX209 group, but the difference was not significant (P=0.0803; Fig. 2E). By contrast, in scene 2, mice in the VPA group spent more time in the cage containing stranger 1 than mice in the control group (P<0.0001) and VPA + STX209 group (P<0.0001) (Fig. 2F). Notably, there were no significant differences among the mice of the four groups in scene 2 with regard to total time in both cages (Fig. 2G).

Moreover, the SPI of VPA model mice was lower than that of mice in the control group (P<0.0001); after STX209 treatment, the SPI of VPA model mice was significantly increased (P<0.0001) (Fig. 2H). These results revealed that VPA mice exhibited social novelty deficits, whereas STX209 treatment ameliorated the deficits of VPA mice.

STX209 ameliorates the novelty recognition deficits of VPA model mice. Similar to previous reports of other ASD model mice (40), VPA model mice exhibited novel object preference deficits compared with the control mice, as demonstrated by VPA model mice spending less time in regions containing the familiar objects in scene 1 and the novel object in scene 2; scene 1, P=0.0042; scene 2, P<0.0001; Fig. 3C and D). Chronic STX209 treatment increased the amount of time VPA model mice spent in the region containing the novel object (scene 1, P=0.0125; scene 2, P=0.0005; Fig. 3A-D). The DI is a valuable index that reflects object recognition memory and preference

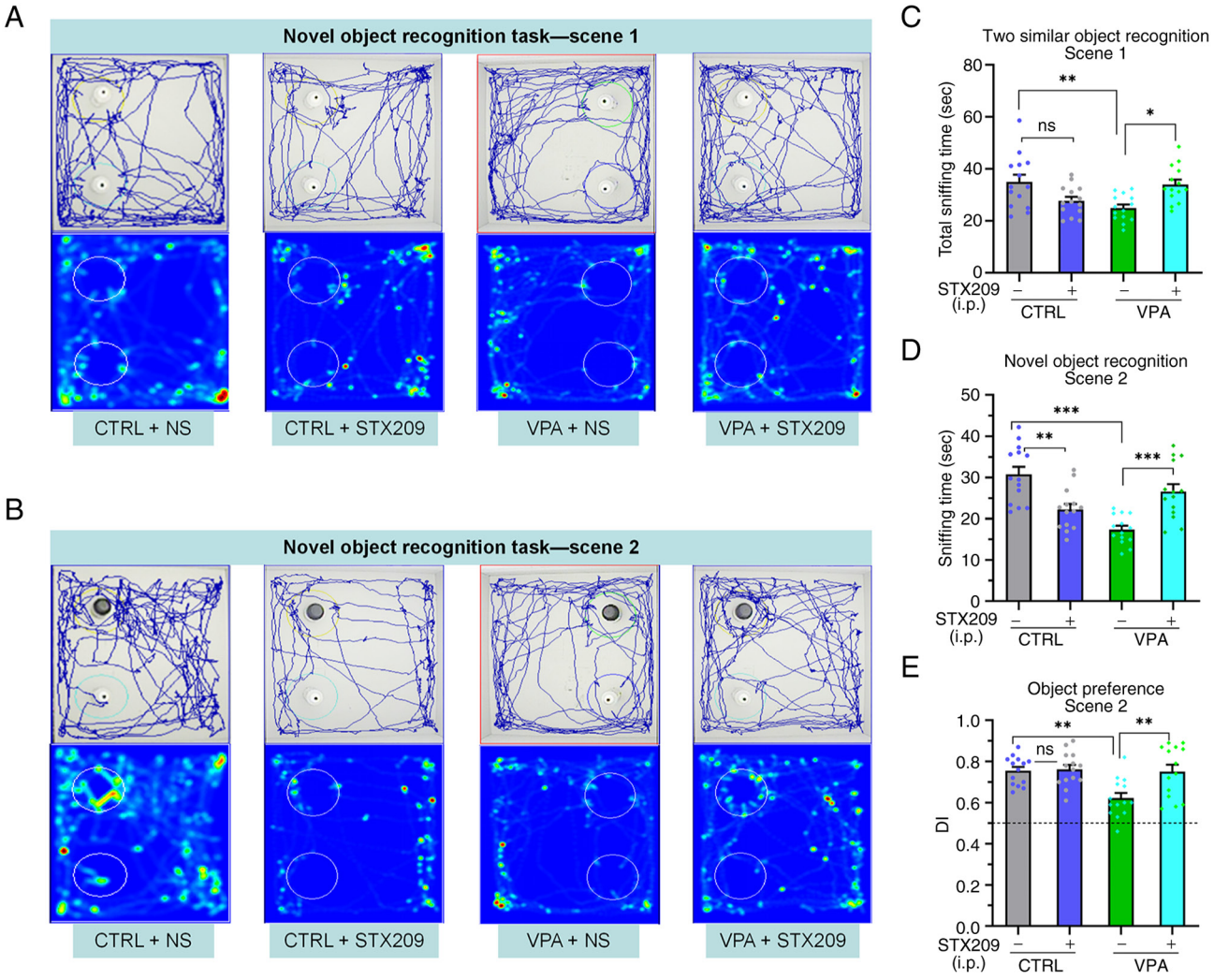

Figure 3. STX209 ameliorates the novelty recognition deficits of VPA model mice. (A) Representative trace and heatmap images from tested mice in scene 1 in the novel object recognition task. (B) Representative trace and heatmap images from tested mice in scene 2 in the novel object recognition task. This test was used to assess novelty recognition ability. (C) Total time spent sniffing the two similar objects by each group of mice in scene 1. (D) Time spent sniffing the novel object by each group of mice in scene 2. (E) DI of each group of mice in scene 2. *P<0.05, **P<0.01, ***P<0.001 (two-way ANOVA followed by Bonferroni post hoc test). All data are presented as the mean ± SEM. Each group had 14 mice. CTRL, control; DI, discrimination index; NS, normal saline; VPA, valproic acid; ns, no significance.

for novel objects. The results revealed that the DI of the VPA group mice was lower than that of the control group mice (P=0.0030) and VPA + STX209 group mice (P=0.0043) (Fig. 3E). These results revealed that STX209 treatment ameliorated the novel object preference deficits of VPA model mice.

In addition, STX209 caused a reduction in the time control mice spent exploring the novel object in scene 2 (control vs. control + STX209, P=0.0015; Fig. 3D), but it did not significantly affect the DI (P>0.9999; Fig. 3E), indicating that STX209 affected only the sniffing time in control mice but had no effect on the preference for novel objects.

STX209 ameliorates the locomotion and exploration activity deficits of VPA model mice. In the open-field task (task 1), VPA model mice exhibited reduced locomotion and exploratory behaviour compared with control mice, as determined by decreases in the time travelled in the inner area (P<0.0001; Fig. 4A and C), the distance travelled in the inner area (P<0.0001; Fig. 4D) and the OFEI (P<0.0001; Fig. 4E). STX209 did not exhibit a positive effect on ameliorating locomotion or exploratory behaviour in VPA mice (P>0.9999, Fig. 4C; P>0.9999, Fig. 4D; P>0.9999, Fig. 4E).

Inspired by a previous study (40), the open-field habituation task (task 2; two tasks spaced 24 h apart) was redesigned to further evaluate the therapeutic effect of STX209. As Fig. 4B showed, in contrast to task 1, mice in the control group and VPA + STX209 group exhibited an increase in locomotion behaviour in task 2 (control group, P<0.0001; VPA + STX209 group, P<0.0001; Fig. 4D), although VPA model mice did not (P=0.9217; Fig. 4D). In addition, in task 2, STX209 treatment had a positive role in ameliorating the exploratory activity deficits of VPA model mice (P<0.0001, Fig. 4C; P<0.0001, Fig. 4D; P<0.0001, Fig. 4E).

The difference in the results of the two tasks may have been related to a decrease in anxiety and fear, which may have been caused by previous experience exploring the same apparatus and familiarity with the environment. Therefore,

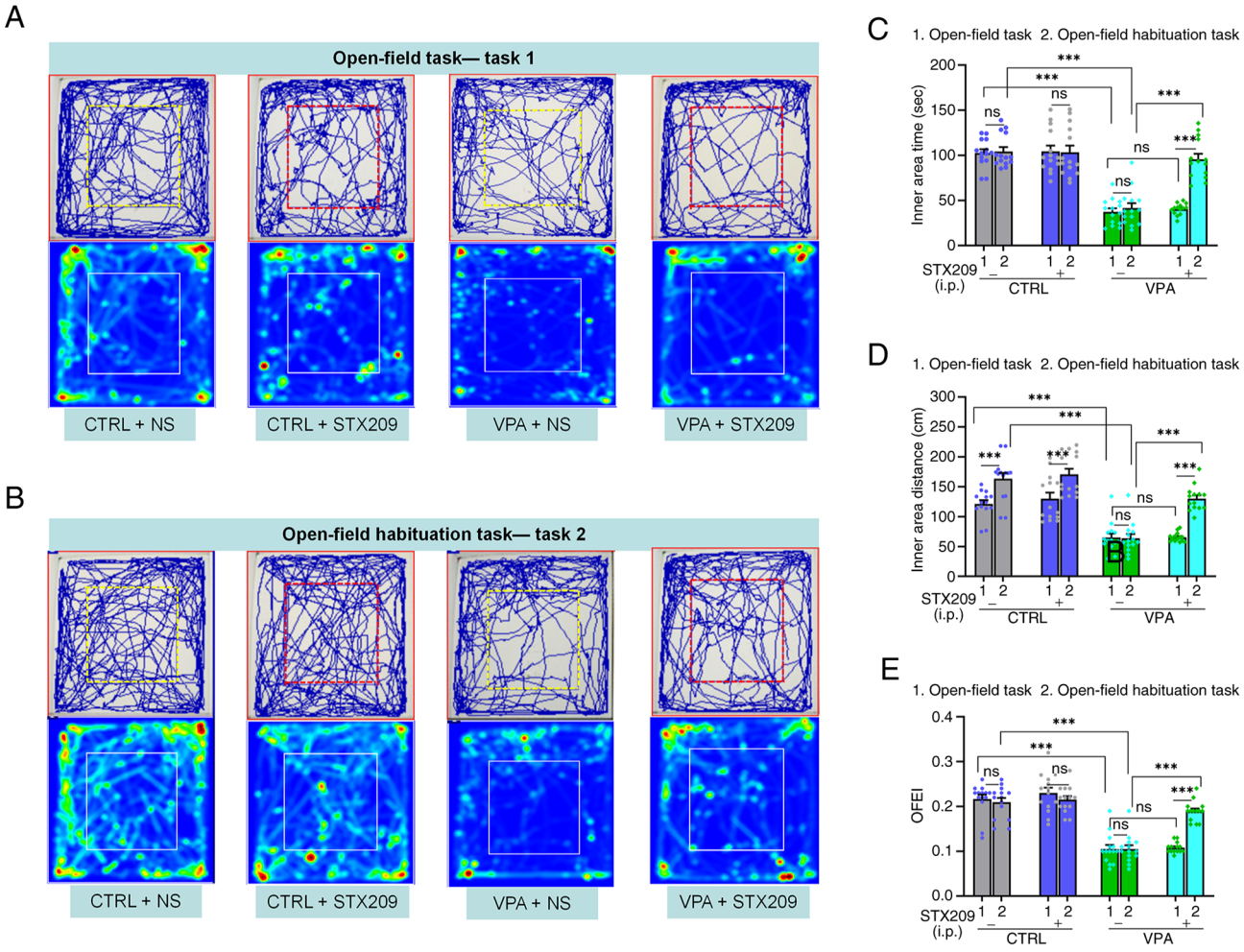

Figure 4. STX209 ameliorates the locomotion and exploratory activity deficits of VPA model mice. (A) Representative trace and heatmap images from tested mice in the open-field task (task 1). (B) Representative trace and heatmap images from tested mice in the open-field habituation task (task 2). (C) Time travelled in the inner zone by mice in the two open-field tasks. (D) Distance travelled by mice in the inner zone in the two open-field tasks. (E) OFEI of mice in the two open-field tasks. ***P<0.001 (Student's paired t-test was used to compare the differences in behaviour in every group of mice between the two tasks, and three-way mixed ANOVA followed by Bonferroni post hoc test was used to compare the difference in same task among four group). All data are presented as the mean ± SEM. Each group had 14 mice. CTRL, control; OFEI, open-field exploration index; NS, normal saline; VPA, valproic acid; ns, no significance.

treatment with STX209 markedly ameliorated the deficit of the VPA model mice in recognizing a familiar environment in the open-field habituation task.

Treatment with STX209 ameliorates the marble-burying deficits in VPA model mice. As shown in Fig. 5A, the numbers of buried marbles and burying actions were smaller in the VPA group compared with in the control group (P<0.0001, Fig. 5B; P<0.0001, Fig. 5C), indicating that VPA model mice have marble-burying deficits. Chronic STX209 treatment increased these parameters in the VPA group (P<0.0001, Fig. 5B; P<0.0001, Fig. 5C), indicating that STX209 had a certain therapeutic effect on the marble-burying deficit of VPA model mice.

In addition, STX209 inhibited marble burying in control mice (control group vs. control + STX209 group, P<0.0001, Fig. 5B; P<0.0001, Fig. 5C). This result may be related to the fact that GABABR2 agonists are anti-anxiety drugs and that selective inhibition of burying behaviour in rodents is thought to be an effect of anti-anxiety drugs, which is consistent with a previous study (36).

Linear correlation between the number of buried marbles and the number of burying actions. The number of marbles buried and the burying actions of all groups of mice were counted and linear regression between them was determined (P<0.0001, r^2=0.9558/y=9.653 * x + 7.735; Fig. 5D). This showed that the marble burying actions in the test were effective, and the time of test is appropriate.

Prenatal VPA exposure causes rearrangement of neuronal dendrites and spines in the hippocampi of VPA model mice, and STX209 ameliorates these neuronal structural defects. Compared with in the control group, Sholl analysis indicated that the total dendritic length of neurons in the dentate gyrus (DG) region was reduced in the VPA model group (P<0.0001; Fig. 6A and B), indicating neuronal development defects in VPA model mice. Chronic administration of STX209 ameliorated dendritic length (P<0.0001; Fig. 6B). Quantitative morphological analysis of showed that compared with the control group, density of total spines and mushroom spines at the basal dendritic terminals of pyramidal neurons in the hippocampal DG region were increased in the VPA

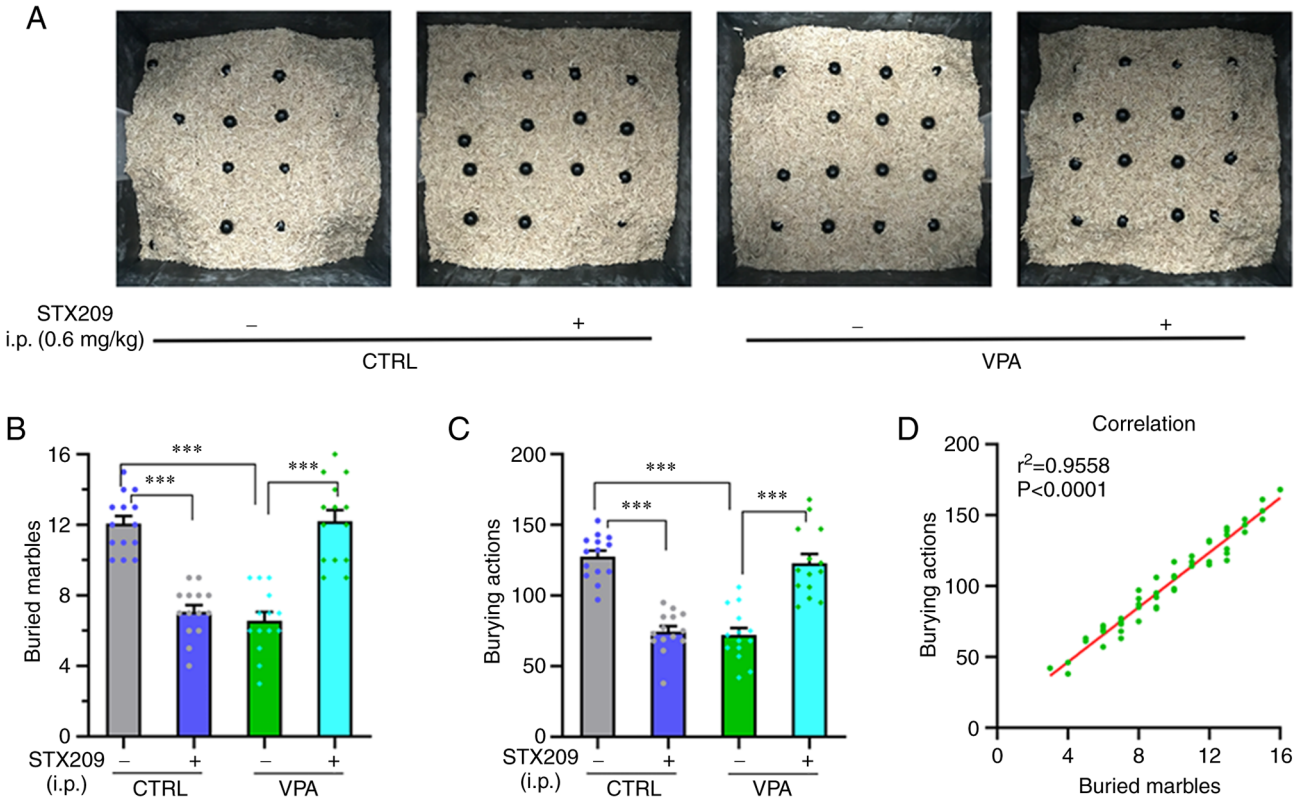

Figure 5. STX209 ameliorates marble burying deficits in VPA model mice. (A) Representative marble burying maps. (B) Numbers of buried marbles of each group of mice in the 10-min test. (C) Number of burying actions (strong and obvious digging or burial movement) for each group of mice in the 10-min test. ***P<0.001 (two-way ANOVA followed by Bonferroni post hoc test). All data are presented as the mean ± SEM. Each group had 14 mice. (D) Correlation analysis between the number of buried marbles and the number of burying actions was conducted using Pearson correlation analysis and linear regression analysis. All mice (n=56) were included in the analysis, and there was a linear correlation between the number of buried marbles and the number of burying actions. CTRL, control; VPA, valproic acid.

model group (P<0.0001, Fig. 6C and G; P=0.0008, Fig. 6H), indicating that neuronal connectivity in DG region of VPA model mice was abnormally increased. Chronic administration of STX209 ameliorated the defects in total spine density (P=0.0006; Fig. 6G) in VPA model mice; however, STX209 did not exhibit a significant difference in ameliorating the defects of mushroom spine density (P=0.1679; Fig. 6H).

Similar to neuronal dendrites in the DG region, as Fig. 6D showed, the total dendritic length of neurons in the CA1 region in the VPA model group was also reduced compared with in the control group (P<0.0001; Fig. 6E). Chronic administration of STX209 ameliorated the reduction in dendritic length (P=0.0009; Fig. 6E) in VPA model mice. Unlike that in the DG region (Fig. 6F), compared with in the CTRL group, density of total spines and mushroom spines at the basal dendritic terminals of pyramidal neurons in the hippocampal CA1 region were decreased in the VPA group (P<0.0001, Fig. 6I; P<0.0001, Fig. 6J), indicating that the neuronal connectivity in CA1 region of VPA model mice was abnormally decreased. Chronic administration of STX209 also ameliorated this defect (P<0.0001, Fig. 6J; P=0.0007, Fig. 6K) in VPA model mice.

In conclusion, examination of hippocampal morphology in this animal model revealed that VPA exposure *in utero* altered the dendritic morphology and dendritic spine number of neurons in the CA1 and DG regions of the hippocampus in offspring. The dendritic arbors of neurons in the CA1 and DG regions in the VPA model mice were dysplastic, and the total dendritic length was abnormal. Chronic administration of STX209 ameliorated these neuronal structural defects in VPA model mice.

STX209 ameliorates GABAergic system impairment in VPA model mice. According to the results of western blot analysis (Fig. 7A and B), the protein expression levels of GAD65/67 and GABABR2 were decreased in the hippocampus of VPA model mice compared with those in control mice (GABABR2, P<0.0001, Fig. 7C; GAD65/67, P=0.0071, Fig. 7D). By contrast, STX209 treatment increased the expression levels of GABABR2 in VPA model mice (P=0.0010, Fig. 7C), although it did not increase the expression levels of GAD65/67 (P>0.9999, Fig. 7D). These results suggested that prenatal VPA exposure may lead to dysregulation of the hippocampal GABAergic system in the brains of offspring mice. After chronic administration of STX209, the ability of the hippocampal GABAergic system to produce GABA did not improve, but the GABAergic pathway transduction ability was enhanced.

Discussion

To the best of our knowledge, the present preclinical study is the first to focus on the potential use of the GABABR2 agonist STX209 as a treatment for VPA model mice; this model is used for simulating children with ASD who were exposed

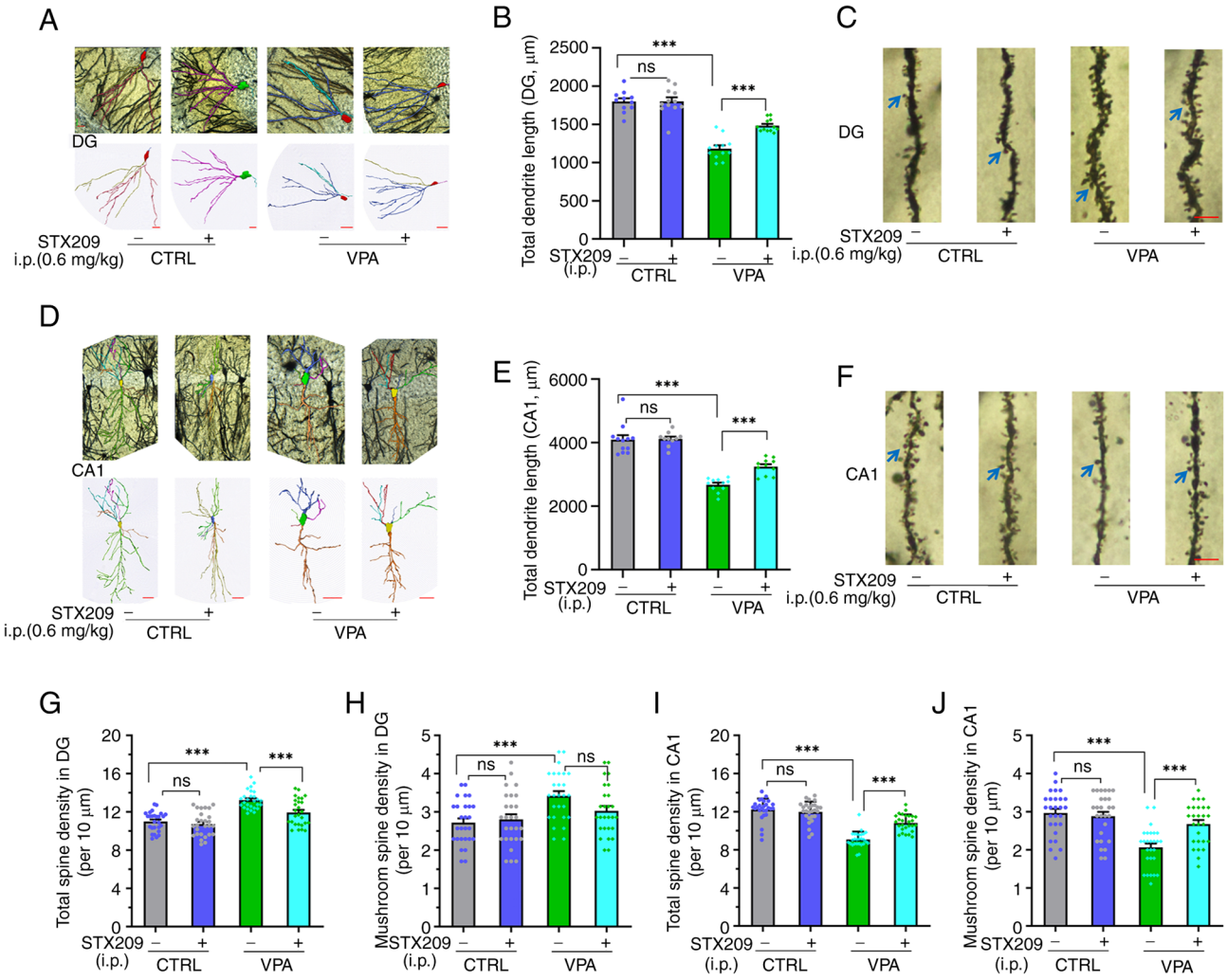

Figure 6. Prenatal VPA exposure impairs neuronal development in the DG/CA1 in the hippocampi of offspring mice and STX209 ameliorates these neuronal structural defects. Representative reconstructions of the dendrites of (A) DG and (D) CA1 neurons in the hippocampus in the four groups (scale bar, 50 μm), concentric circles are 5 μm apart. Representative maps of dendritic spines at the ends of basal dendrites (tertiary dendrites) of (C) DG and (F) CA1 neurons in the four groups of mice. Arrows indicate the mushroom spine (scale bar, 5 μm). Total length of dendrites of (B) DG and (E) CA1 neurons in the four groups. Density of (G and I) total spines and (H and J) mushroom spines at the end of the basal dendrites (tertiary dendrites) of pyramidal neurons in the DG and CA1 regions of the hippocampus of the four groups (n=27/group). ***P<0.001 (two-way ANOVA followed by Bonferroni post hoc test). All data are presented as the mean ± SEM. CTRL, control; DG, dentate gyrus; VPA, valproic acid; ns, no significance.

to VPA *in utero*. In the present study, STX209 significantly ameliorated core autism-like behaviours in VPA model mice. The possible mechanism underlying the behavioural improvement in VPA model mice may have involved the amelioration of alterations in the structure and function of the hippocampus, including promotion of neuronal growth and remodelling, synapse formation, and pruning and improvement of GABAergic pathway function.

Based on the multifactorial aetiology and complex pathophysiology of ASD, there is no animal model that can capture, at once, all of the molecular, cellular and behavioural features of ASD. Moreover, ASD is defined by specific behavioural characteristics, and an important method in its research is to focus on animal behaviours related to the core diagnostic symptoms of the disease to study both the underlying neural mechanisms and potential pharmacological targets to ameliorate autism type (4,32). The robustness of the behavioural alterations and the neural/molecular changes revealed support the VPA model mice as a reliable tool for investigating the neural basis of social disorders (4,5,8,9), which has been widely used in preclinical studies of ASD (8). In the present study, a modified method was used to generate VPA model mice (49). The modelling success rate was satisfactory (the failed pregnancy was only 10.5%) and the mice had obvious phenotypes, such as delayed weight development, a 100% tail deformity rate and neurodevelopmental delay (24,49,53). Furthermore, the behavioural tests conducted confirmed that the model mice exhibited obvious autism-like behaviour. Regarding the dosage of STX209, according to the principle of selecting the minimum effective dose, we selected the minimum dose supported by the reference (36,41,42) that can fully activate the gabab receptor. A previous study indicated that administration of STX209 in the drinking water at 0.5 mg/ml could provide average brain exposure equivalent to 6 mg/kg administered by intraperitoneal injection twice a day, which was sufficient to engage GABABR2 and reduce excessive protein synthesis in Fmr1$^{-/y}$ mice and to correct the excess dendritic spine phenotype of Fmr1-deficient mice (36). This previous study

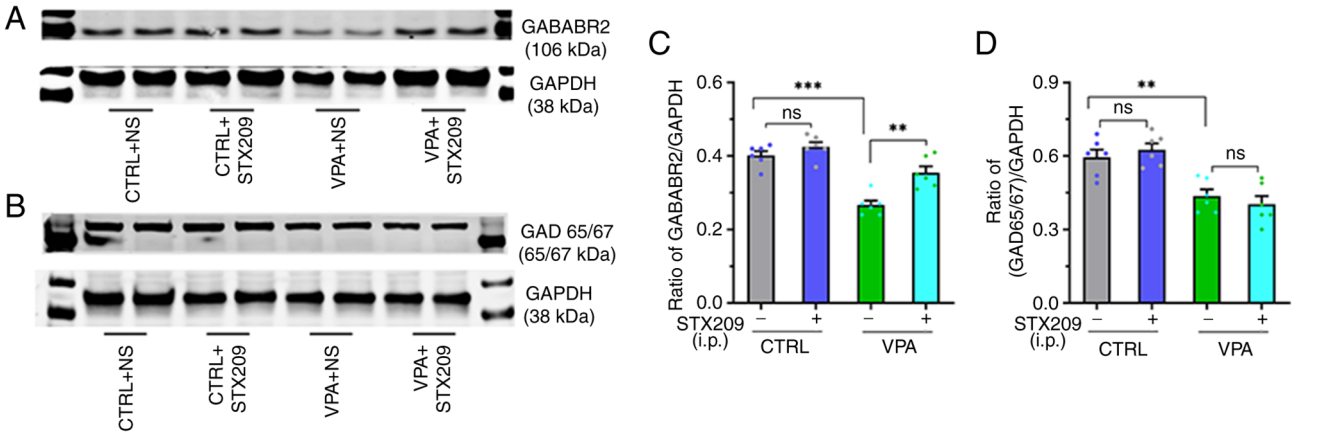

Figure 7. Prenatal VPA exposure causes GABAergic system function defects in the hippocampus of VPA model mice, and nervous system damage in the CA1 and DG regions of the hippocampus in the mice. STX209 ameliorates these defects. Representative western blotting images showing the expression levels of (A) GABABR2 and (B) GAD65/67 protein in the entire hippocampus in each group. Histograms of the relative expression levels of (C) GABABR2 and (D) GAD65/67 proteins in each group (n=3 mice from different mothers/group; western blotting was repeated once). Chronic administration of STX209 did not increase GAD65/67 expression in VPA model mice but elevated the expression level of GABABR2. **P<0.01, ***P<0.001 (two-way ANOVA followed by Bonferroni post hoc test). All data are presented as the mean ± SEM. CTRL, control; NS, normal saline; GABABR2, γ-aminobutyric acid type B receptor 2; GAD65/67, glutamic acid decarboxylase 65/67; VPA, valproic acid; ns, no significance.

also demonstrated that acute intraperitoneal administration of STX209 significantly reduced the percentage of mice displaying seizures (seizure incidence), with a minimum effective dose of 1.5 mg/kg (36). Another study revealed that STX209 could suppress audiogenic seizures in Fmr1-knockout mice on a seizure-resistant C57BL/6 background with an effective dose of 1.0 mg/kg (single doses) (41). A clinical trial in patients with fragile X syndrome also showed a benefit of STX209 in children aged 6-11 (~0.66 mg/kg/day) (42). Therefore, a minimum dosage at which the drug can fully stimulate the GABABR2 (0.6 mg/kg, intraperitoneal administration, twice a day; total dose, 1.2 mg/day) was chosen for the present study.

The social interaction test is a widely used, standardized test for assessing social interaction deficits, which is often used to evaluate general sociability in rodents (4,8,58,59). The other behavioural tests used for sociability include the youth play behaviour test and social (play) behaviour test (40). Based on the procedures of these simple tests, the behaviour of tested mice are easily affected by the other mice during interaction and the various quantitative parameters make their evaluation highly subjective. Therefore only the three-chamber test was used for evaluating the sociability of tested mice in the present study. The results indicated that STX209 treatment ameliorated sociability deficits and preference for social novelty deficits in VPA model mice.

Restrictive interest is another core symptom of ASD, and the novel object recognition task revealed that STX209 ameliorated object recognition memory and preference for the novel object in VPA model mice. Characteristics associated with ASD include anxiety, epileptic seizures and cognitive impairment, anxiety is one of the most common comorbid conditions in patients (8,9). Furthermore, in the present study, VPA model mice exhibited obvious locomotion and exploratory behavioural deficits in the open-field task and open-field habituation task, which could be improved by STX209. Following STX209 treatment, VPA mice exhibited reduced anxiety and stronger exploratory characteristic behaviour in the open-field habituation task.

Repetitive behaviour is another characteristic phenotype of VPA model mice and a defining symptom of ASD. The marble burying test is regarded as an assessment of perseverative/repetitive behaviour in mice. Previous studies assessing marble burying or digging bouts have confirmed increased stereotyped, perseverative/repetitive behaviours in VPA-exposed animals (50,60). The original purpose of designing this test was to observe the perseverative/repetitive behaviour of VPA model mice; however, the results of the present study demonstrated that VPA model mice exhibited fewer digging and burying actions, and buried fewer marbles than control mice. Notably, STX209 improved these phenotypes. These unanticipated results may be because the marble burying test itself is a robust test model for identifying anxiolytics (61-63) in the anxiolytic model, glass marbles are seen as an unfamiliar and potentially threatening object, and the burying of marbles by the mice to remove the threat is considered a sign of an instinctive anxiety-like response. This behavior is called 'conditioned defensive burying', which is an adaptation to a new complex environment (61-63). The results of present study further support the suggestion that burying marbles is a manifestation of an instinctive anxiety-like response. STX209 rescued the defect of conditioned defensive burial in VPA model mice, which may be associated with beneficial effects of long-term STX209 administration on nervous system development in VPA mice.

After demonstrating that STX209 was able to improve autism-like behaviour in VPA model mice, the present study focused on hippocampal structure. The Golgi-Cox impregnation method is a powerful neuromorphological staining tool that has been widely used to obtain valuable information regarding neural morphology and to quantitatively assess parameters, such as dendritic spine number, dendritic length and branching complexity. The present study evaluated neuronal morphology and dendritic spine development in the hippocampus of the mice by Golgi staining to assess their synaptic plasticity status. Consistent with previous reports and the aforementioned behavioural data, neuronal

development was disrupted in the hippocampal CA1 regions in mice exposed to VPA *in utero* (33,64,65). Quantitative morphological analysis of dendritic spine density revealed that the total spine and mushroom spine density at the end of the basal dendrites of pyramidal neurons in the CA1 region of the hippocampus were decreased, but that the density of spines at the end of dendrites in the DG region was increased. These results suggested that VPA model mice had hypoconnectivity in the CA1 region and hyperconnectivity in the DG region. In addition, the results revealed that STX209 altered the morphology, total spine and mushroom spine density (although this was not statistically significant) of neurons in CA1 and the morphology, total spine density of neurons in DG regions in the VPA model hippocampus so that they were more similar to those in the control group. The CA1 and DG regions are the main components of the classic trisynaptic circuit (entorhinal cortex→DG→CA3→CA1→subiculum), which has been reported to be closely related to memory and to be an important basis of hippocampal function (66,67). In VPA model mice, the abnormal dendritic morphology and hypoconnectivity in the CA1 region of the hippocampus, as well as the morphological defects and local hyperconnectivity in the DG region, may cause trisynaptic circuit disorder and E-I imbalance, thus affecting the cognitive processes of learning and memory associated with navigation, exploration and locomotion. According to this finding, it was hypothesized that activation of GABABR2 by STX209 may ameliorate neuronal developmental defects in the CA1 and DG regions of the hippocampus in VPA model mice, normalize signal transduction in the hippocampus and contribute to achieving E-I rebalance. This conclusion is supported by several mouse models of E-I dysfunction (22,68).

To further explore the mechanisms involved, GAD65/67 and GABABR2 protein expression levels in the hippocampus in each group were assessed, and it was revealed that the expression levels of both proteins were decreased in VPA model mice. STX209 increased GABABR2 protein expression levels, but did not increase GAD65/67 protein expression in the hippocampus. GAD65/67 are the key enzymes in GABA biosynthesis, and GABABR2 is the site of action of STX209 and GABA. Furthermore, GAD65/67 are joint nodes of the GABAergic system (69,70). The present findings revealed that exposure to VPA *in utero* caused hippocampal GABAergic system functional defects in offspring mice and that chronic STX209 administration did not improve GABA production capacity in VPA model mice but did increase GABAergic pathway function. GABABR is indispensable for regulating the development of neural networks. Studies have reported that GABA and its receptors serve a classic role in neurodevelopment and synaptic plasticity, and can regulate almost all of the key steps of neuronal network formation, and GABABR dysfunction may cause behavioural defects in ASD (71,72). Chronic administration of a low dose of STX209 during the growth phase in VPA model pups most likely activated GABABR, thus compensating for the lack of GABA, and then produced a series of physiological responses, such as promotion of hippocampal neuron survival, migration and dendritic development in VPA model pups, and correction of the formation and pruning of dendritic spines. This compensatory mechanism may contribute to maintaining the stability and functionality of neural circuits in the face of challenges posed by developmental events in this animal model, thereby ameliorating the ASD-related behaviours of mice exposed to VPA *in utero*.

In conclusion, the present study provided strong evidence that pharmacologically enhancing GABA signalling may be a promising strategy for the treatment of VPA model mice. While the experimental results are encouraging, the limitations of the study are that it is impossible to replicate the complex genetic and environmental conditions of children with ASD due to the homogeneity between experimental animals and the same experimental environment. Furthermore, the present study only used the exploratory drug, STX209, and lacked the use of a known GABABR2 agonist to test as a positive control, and also lacked measurement of GABABR signalling activity. Furthermore, STX209 cannot completely cross the blood-brain barrier; therefore, this is another limitation of this drug. However, the results indicated the possibility of early intervention with STX209, an exploratory GABABR2 agonist, for the treatment of children with ASD. In addition, the results of the present study supported that GABABR is a promising drug target for the treatment of neuropsychiatric disorders and developmental disorders, which may be an important direction for the development of novel drugs for ASD treatment.

Acknowledgements

The authors would like to thank the Ningxia Key Laboratory of Cerebrocranial Disease for technical support (special thanks to Mrs. Zhang Chun for her help in cryopreservation of mouse brain tissue); Mr. Zhang Xian and Mr. Hao Xiaoyan (Ningxia Medical University) for their assistance during the experiment; and Mrs. Liu Li and Mrs. Yang Dan (Neuroscience of the Public Technology Platform of School of Medicine, Zhejiang University) for their help in analysing the results of the Golgi-Cox staining.

Funding

This study was supported by the National Natural Science Foundation of China (NSFC) (grant no. 82060261), the Key Research Project of Ningxia (grant no. 2018YBZD04917) and the Ningxia Hui Autonomous Region '13th Five-Year Plan' Major Science and Technology Projects (Ningxia Brain Project) (grant no. 2016BZ07).

Availability of data and materials

The datasets used and/or analysed during the current study are available from the corresponding author on reasonable request.

Authors' contributions

All authors contributed to the study conception and design. Senior authors FW and TS are accountable for all aspects of the work in ensuring that questions related to the accuracy or integrity of any part of the work are appropriately investigated and resolved. SJ, LX and YS made major contributions to the conception, design and the acquisition, analysis, or interpretation of data for the work. Material preparation, experiments

and data collection were performed by MH, CG, CZ, HC, JD, WL and YW. The first draft of the manuscript was written by SJ and all authors commented on previous versions of the manuscript. All authors read and approved the final manuscript. SJ and FW confirm the authenticity of all the raw data.

Ethics approval and consent to participate

All mice were handled according to protocols approved by the Institutional Animal Care and Use Committee of Ningxia Medical University (IACUC Animal Use Certificate No. 2019-152). All efforts were made to minimize the number of animals used and their suffering.

Patient consent for publication

Not applicable.

Competing interests

The authors declare that they have no competing interests.

References

1. American Psychiatric Association: Diagnostic and statistical manual of mental disorders: DSM-5™ (5th edition). American Psychiatric Publishing, Washington, DC, 2013.
2. Volkmar FR, Woodbury-Smith M, Macari SL and Øien RA: Seeing the forest and the trees: Disentangling autism phenotypes in the age of DSM-5. Dev Psychopathol 33: 625-633, 2021.
3. Christensen DL, Maenner MJ, Bilder D, Constantino JN, Daniels J, Durkin MS, Fitzgerald RT, Kurzius-Spencer M, Pettygrove SD, Robinson C, *et al*: Prevalence and characteristics of autism spectrum disorder among children aged 4 years-early autism and developmental disabilities monitoring network, seven sites, United States, 2010, 2012, and 2014. MMWR Surveill Summ 68: 1-19, 2019.
4. Servadio M, Vanderschuren LJ and Trezza V: Modeling autism-relevant behavioral phenotypes in rats and mice: Do 'autistic' rodents exist? Behav Pharmacol 26: 522-540, 2015.
5. Roullet FI, Lai JK and Foster JA: In utero exposure to valproic acid and autism-a current review of clinical and animal studies. Neurotoxicol Teratol 36: 47-56, 2013.
6. Taleb A, Lin W, Xu X, Zhang G, Zhou QG, Naveed M, Meng F, Fukunaga K and Han F: Emerging mechanisms of valproic acid-induced neurotoxic events in autism and its implications for pharmacological treatment. Biomed Pharmacother 137: 111322, 2021.
7. Chaste P and Leboyer M: Autism risk factors: Genes, environment, and gene-environment interactions. Dialogues Clin Neurosci 14: 281-292, 2012.
8. Tartaglione AM, Schiavi S, Calamandrei G and Trezza V: Prenatal valproate in rodents as a tool to understand the neural underpinnings of social dysfunctions in autism spectrum disorder. Neuropharmacology 159: 107477, 2019.
9. Nicolini C and Fahnestock M: The valproic acid-induced rodent model of autism. Exp Neurol 299: 217-227, 2018.
10. Schneider T, Roman A, Basta-Kaim A, Kubera M, Budziszewska B, Schneider K and Przewłocki R: Gender-specific behavioral and immunological alterations in an animal model of autism induced by prenatal exposure to valproic acid. Psychoneuroendocrinology 33: 728-740, 2008.
11. McPheeters ML, Warren Z, Sathe N, Bruzek JL, Krishnaswami S, Jerome RN and Veenstra-Vanderweele J: A systematic review of medical treatments for children with autism spectrum disorders. Pediatrics 127: e1312-e1321, 2011.
12. Owen R, Sikich L, Marcus RN, Corey-Lisle P, Manos G, McQuade RD, Carson WH and Findling RL: Aripiprazole in the treatment of irritability in children and adolescents with autistic disorder. Pediatrics 124: 1533-1540, 2009.
13. Eissa N, Al-Houqani M, Sadeq A, Ojha SK, Sasse A and Sadek B: Current enlightenment about etiology and pharmacological treatment of autism spectrum disorder. Front Neurosci 12: 304, 2018.
14. Canitano R: New experimental treatments for core social domain in autism spectrum disorders. Front Pediatr 2: 61, 2014.
15. Hashemi E, Ariza J, Rogers H, Noctor SC and Martínez-Cerdeño V: The number of parvalbumin-expressing interneurons is decreased in the prefrontal cortex in autism. Cereb Cortex 27: 1931-1943, 2017.
16. Ariza J, Rogers H, Hashemi E, Noctor SC and Martínez-Cerdeño V: The number of chandelier and basket cells are differentially decreased in prefrontal cortex in autism. Cereb Cortex 28: 411-420, 2018.
17. Fatemi SH, Folsom TD, Reutiman TJ and Thuras PD: Expression of GABA(B) receptors is altered in brains of subjects with autism. Cerebellum 8: 64-69, 2009.
18. Fatemi SH, Folsom TD and Thuras PD: Deficits in GABA(B) receptor system in schizophrenia and mood disorders: A post-mortem study. Schizophr Res 128: 37-43, 2011.
19. Fatemi SH, Halt AR, Stary JM, Kanodia R, Schulz SC and Realmuto GR: Glutamic acid decarboxylase 65 and 67 kDa proteins are reduced in autistic parietal and cerebellar cortices. Biol Psychiatry 52: 805-810, 2002.
20. Oblak AL, Gibbs TT and Blatt GJ: Reduced GABAA receptors and benzodiazepine binding sites in the posterior cingulate cortex and fusiform gyrus in autism. Brain Res 1380: 218-228, 2011.
21. Oblak AL, Gibbs TT and Blatt GJ: Decreased GABA(B) receptors in the cingulate cortex and fusiform gyrus in autism. J Neurochem 114: 1414-1423, 2010.
22. Han S, Tai C, Westenbroek RE, Yu FH, Cheah CS, Potter GB, Rubenstein JL, Scheuer T, de la Iglesia HO and Catterall WA: Autistic-like behaviour in Scn1a+/- mice and rescue by enhanced GABA-mediated neurotransmission. Nature 489: 385-390, 2012.
23. Lee E, Lee J and Kim E: Excitation/inhibition imbalance in animal models of autism spectrum disorders. Biol Psychiatry 81: 838-347, 2017.
24. Hou Q, Wang Y, Li Y, Chen D, Yang F and Wang S: A developmental study of abnormal behaviors and altered GABAergic signaling in the VPA-treated rat model of autism. Front Behav Neurosci 12: 182, 2018.
25. Banerjee A, García-Oscos F, Roychowdhury S, Galindo LC, Hall S, Kilgard MP and Atzori M: Impairment of cortical GABAergic synaptic transmission in an environmental rat model of autism. Int J Neuropsychopharmacol 16: 1309-1318, 2013.
26. Chau DK, Choi AY, Yang W, Leung WN and Chan CW: Downregulation of glutamatergic and GABAergic proteins in valproric acid associated social impairment during adolescence in mice. Behav Brain Res 316: 255-260, 2017.
27. Rinaldi T, Silberberg G and Markram H: Hyperconnectivity of local neocortical microcircuitry induced by prenatal exposure to valproic acid. Cereb Cortex 18: 763-770, 2008.
28. Rinaldi T, Perrodin C and Markram H: Hyper-connectivity and hyper-plasticity in the medial prefrontal cortex in the valproic acid animal model of autism. Front Neural Circuits 2: 4, 2008.
29. Lenart J, Augustyniak J, Lazarewicz JW and Zieminska E: Altered expression of glutamatergic and GABAergic genes in the valproic acid-induced rat model of autism: A screening test. Toxicology 440: 152500, 2020.
30. Norton SA, Gifford JJ, Pawlak AP, Derbaly A, Sherman SL, Zhang H, Wagner GC and Kusnecov AW: Long-lasting behavioral and neuroanatomical effects of postnatal valproic acid treatment. Neuroscience 434: 8-21, 2020.
31. Schiavi S, Iezzi D, Manduca A, Leone S, Melancia F, Carbone C, Petrella M, Mannaioni G, Masi A and Trezza V: Reward-related behavioral, neurochemical and electrophysiological changes in a rat model of autism based on prenatal exposure to valproic acid. Front Cell Neurosci 13: 479, 2019.
32. Crawley JN: Translational animal models of autism and neurodevelopmental disorders. Dialogues Clin Neurosci 14: 293-305, 2012.
33. Bringas ME, Carvajal-Flores FN, López-Ramírez TA, Atzori M and Flores G: Rearrangement of the dendritic morphology in limbic regions and altered exploratory behavior in a rat model of autism spectrum disorder. Neuroscience 241: 170-187, 2013.
34. Lal R, Sukbuntherng J, Tai EH, Upadhyay S, Yao F, Warren MS, Luo W, Bu L, Nguyen S, Zamora J, *et al*: Arbaclofen placarbil, a novel R-baclofen prodrug: Improved absorption, distribution, metabolism, and elimination properties compared with R-baclofen. J Pharmacol Exp Ther 330: 911-921, 2009.

35. Sanchez-Ponce R, Wang LQ, Lu W, von Hehn J, Cherubini M and Rush R: Metabolic and pharmacokinetic differentiation of STX209 and racemic baclofen in humans. Metabolites 2: 596-613, 2012.
36. Henderson C, Wijetunge L, Kinoshita MN, Shumway M, Hammond RS, Postma FR, Brynczka C, Rush R, Thomas A, Paylor R, *et al*: Reversal of disease-related pathologies in the fragile X mouse model by selective activation of GABAB receptors with arbaclofen. Sci Transl Med 4: 152ra128, 2012.
37. Silverman JL, Pride MC, Hayes JE, Puhger KR, Butler-Struben HM, Baker S and Crawley JN: GABAB receptor agonist R-baclofen reverses social deficits and reduces repetitive behavior in two mouse models of autism. Neuropsychopharmacology 40: 2228-2239, 2015.
38. Qin M, Huang T, Kader M, Krych L, Xia Z, Burlin T, Zeidler Z, Zhao T and Smith CB: R-baclofen reverses a social behavior deficit and elevated protein synthesis in a mouse model of fragile X syndrome. Int J Neuropsychopharmacol 18: pyv034, 2015.
39. Sinclair D, Featherstone R, Naschek M, Nam J, Du A, Wright S, Pance K, Melnychenko O, Weger R, Akuzawa S, *et al*: GABA-B agonist baclofen normalizes auditory-evoked neural oscillations and behavioral deficits in the Fmr1 knockout mouse model of fragile X syndrome. eNeuro 4: ENEURO.0380-16.2017, 2017.
40. Stoppel LJ, Kazdoba TM, Schaffler MD, Preza AR, Heynen A, Crawley JN and Bear MF: R-baclofen reverses cognitive deficits and improves social interactions in two lines of 16p11.2 deletion mice. Neuropsychopharmacology 43: 513-524, 2018.
41. Pacey LK, Tharmalingam S and Hampson DR: Subchronic administration and combination metabotropic glutamate and GABAB receptor drug therapy in fragile X syndrome. J Pharmacol Exp Ther 338: 897-905, 2011.
42. Berry-Kravis EM, Hessl D, Rathmell B, Zarevics P, Cherubini M, Walton-Bowen K, Mu Y, Nguyen DV, Gonzalez-Heydrich J, Wang PP, *et al*: Effects of STX209 (arbaclofen) on neurobehavioral function in children and adults with fragile X syndrome: A randomized, controlled, phase 2 trial. Sci Transl Med 4: 152ra127, 2012.
43. Erickson CA, Veenstra-Vanderweele JM, Melmed RD, McCracken JT, Ginsberg LD, Sikich L, Scahill L, Cherubini M, Zarevics P, Walton-Bowen K, *et al*: STX209 (arbaclofen) for autism spectrum disorders: An 8-week open-label study. J Autism Dev Disord 44: 958-964, 2014.
44. Veenstra-VanderWeele J, Cook EH, King BH, Zarevics P, Cherubini M, Walton-Bowen K, Bear MF, Wang PP and Carpenter RL: Arbaclofen in children and adolescents with autism spectrum disorder: A randomized, controlled, phase 2 trial. Neuropsychopharmacology 42: 1390-1398, 2017.
45. Frye RE: Clinical potential, safety, and tolerability of arbaclofen in the treatment of autism spectrum disorder. Drug Healthc Patient Saf 6: 69-76, 2014.
46. Berry-Kravis E, Hagerman R, Visootsak J, Budimirovic D, Kaufmann WE, Cherubini M, Zarevics P, Walton-Bowen K, Wang P, Bear MF and Carpenter RL: Arbaclofen in fragile X syndrome: Results of phase 3 trials. J Neurodev Disord 9: 3, 2017.
47. Boivin GP, Hickman DL, Creamer-Hente MA, Pritchett-Corning KR and Bratcher NA: Review of CO_2 as a euthanasia agent for laboratory rats and mice. J Am Assoc Lab Anim Sci 56: 491-499, 2017.
48. American Veterinary Medical Association. AVMA guidelines for the Euthanasia of animals, 2020 edition, 2020.
49. Zheng W, Hu Y, Chen D, Li Y and Wang S: Improvement of a mouse model of valproic acid-induced autism. Nan Fang Yi Ke Da Xue Xue Bao 39: 718-723, 2019 (In Chinese).
50. Choi CS, Gonzales EL, Kim KC, Yang SM, Kim JW, Mabunga DF, Cheong JH, Han SH, Bahn GH and Shin CY: The transgenerational inheritance of autism-like phenotypes in mice exposed to valproic acid during pregnancy. Sci Rep 6: 36250, 2016.
51. Kazlauskas N, Seiffe A, Campolongo M, Zappala C and Depino AM: Sex-specific effects of prenatal valproic acid exposure on sociability and neuroinflammation: Relevance for susceptibility and resilience in autism. Psychoneuroendocrinology 110: 104441, 2019.
52. Jiménez JA and Zylka MJ: Controlling litter effects to enhance rigor and reproducibility with rodent models of neurodevelopmental disorders. J Neurodev Disord 13: 2, 2021.
53. Wang R, Tan J, Guo J, Zheng Y, Han Q, So KF, Yu J and Zhang L: Aberrant development and synaptic transmission of cerebellar cortex in a VPA induced mouse autism model. Front Cell Neurosci 12: 500, 2018.
54. Heyser CJ: Assessment of developmental milestones in rodents. Curr Protoc Neurosci Chapter 8: Unit 8.18, 2004.
55. Antunes M and Biala G: The novel object recognition memory: neurobiology, test procedure, and its modifications. Cogn Process 13: 93-110, 2012.
56. Modabbernia A, Velthorst E and Reichenberg A: Environmental risk factors for autism: An evidence-based review of systematic reviews and meta-analyses. Mol Autism 8: 13, 2017.
57. Binkerd PE, Rowland JM, Nau H and Hendrickx AG: Evaluation of valproic acid (VPA) developmental toxicity and pharmacokinetics in Sprague-Dawley rats. Fundam Appl Toxicol 11: 485-493, 1988.
58. Yang M, Silverman JL and Crawley JN: Automated three-chambered social approach task for mice. Curr Protoc Neurosci Chapter 8: Unit 8.26, 2011.
59. Rein B, Ma K and Yan Z: A standardized social preference protocol for measuring social deficits in mouse models of autism. Nat Protoc 15: 3464-3477, 2020.
60. Kim KC, Kim P, Go HS, Choi CS, Yang SI, Cheong JH, Shin CY and Ko KH: The critical period of valproate exposure to induce autistic symptoms in Sprague-Dawley rats. Toxicol Lett 201: 137-142, 2011.
61. Dallas T, Pinel JP and Fibiger HC: Conditioned defensive burying: A new paradigm for the study of anxiolytic agents. Pharmacol Biochem Behav 15: 619-626, 1981.
62. Kung'u N and Handley SL: Evaluation of marble-burying behavior as a model of anxiety. Pharmacol Biochem Behav 38: 63-67, 1991.
63. Langer E, Einat H and Stukalin Y: Similarities and dissimilarities in the effects of benzodiazepines and specific serotonin reuptake inhibitors (SSRIs) in the defensive marble burying test: A systematic review and meta-analysis. Eur Neuropsychopharmacol 36: 38-49, 2020.
64. Yamaguchi H, Hara Y, Ago Y, Takano E, Hasebe S, Nakazawa T, Hashimoto H, Matsuda T and Takuma K: Environmental enrichment attenuates behavioral abnormalities in valproic acid-exposed autism model mice. Behav Brain Res 333: 67-73, 2017.
65. Hara Y, Ago Y, Taruta A, Katashiba K, Hasebe S, Takano E, Onaka Y, Hashimoto H, Matsuda T and Takuma K: Improvement by methylphenidate and atomoxetine of social interaction deficits and recognition memory impairment in a mouse model of valproic acid-induced autism. Autism Res 9: 926-939, 2016.
66. Stepan J, Dine J and Eder M: Functional optical probing of the hippocampal trisynaptic circuit in vitro: Network dynamics, filter properties, and polysynaptic induction of CA1 LTP. Front Neurosci 9: 160, 2015.
67. Naber PA, Witter MP and Lopes Silva FH: Networks of the hippocampal memory system of the rat. The pivotal role of the subiculum. Ann N Y Acad Sci 911: 392-403, 2000.
68. Gandal MJ, Sisti J, Klook K, Ortinski PI, Leitman V, Liang Y, Thieu T, Anderson R, Pierce RC, Jonak G, *et al*: GABAB-mediated rescue of altered excitatory-inhibitory balance, gamma synchrony and behavioral deficits following constitutive NMDAR-hypofunction. Transl Psychiatry 2: e142, 2012.
69. Lee B, Zhang Y, Kim Y, Kim S, Lee Y and Han K: Age-dependent decrease of GAD65/67 mRNAs but normal densities of GABAergic interneurons in the brain regions of Shank3-overexpressing manic mouse model. Neurosci Lett 649: 48-54, 2017.
70. Ribak CE and Roberts RC: GABAergic synapses in the brain identified with antisera to GABA and its synthesizing enzyme, glutamate decarboxylase. J Electron Microsc Tech 15: 34-48, 1990.
71. Gaiarsa JL and Porcher C: Emerging neurotrophic role of GABAB receptors in neuronal circuit development. Front Cell Neurosci 7: 206, 2013.
72. Heaney CF and Kinney JW: Role of GABA(B) receptors in learning and memory and neurological disorders. Neurosci Biobehav Rev 63: 1-28, 2016.